

CONTROL OF MECHATRONIC SYSTEMS – COMES TOOLBOX

Burak DEMİREL

School of Electrical Engineering
Automatic Control Laboratory
The Royal Institute of Technology (KTH),
Stockholm, Sweden

Levent GÜVENÇ*

Department of Mechanical Engineering
Mekar Mechatronics Research Laboratories
Istanbul Technical University,
Istanbul, Turkey

ABSTRACT

An interactive software tool based on MATLAB to analyze and design controllers for mechatronic systems is presented in this paper. This toolbox called COMES is a graphical user interface (GUI) to routines for four different control approaches: classical control (lead, lag, PID etc.), preview control, model regulator control and repetitive control. These control approaches have all found widespread use in the practical implementation of controllers for mechatronic systems. The aim is to design a user-friendly toolbox with a well designed graphical user interface (GUI), which hides all calculations from the user as much as possible. Thus, the user can focus on the design and analysis phases through the graphical displays rather than being burdened by the complicated calculations that are involved. The effectiveness of the use of this MATLAB-based toolbox was demonstrated by carrying out some design and simulation studies for several position control applications available in the literature.

1 INTRODUCTION

Computer-Aided engineering offers mechatronics engineers and control engineers an open and extensible environment that can be used to explore, develop and share new algorithms, and build applications for the analysis and simulation of mechatronic systems. Additionally, this approach is well suited for educational purposes as a complement to educational material like text books and laboratory exercises. The students using computer aided control system design tools are able to improve both their design skills and insight into control theory. Furthermore, these tools allow students to work at home.

Many tools for control education and engineering design have been developed for several years. For example, Schaufelberger and his team [1] have developed many interesting ideas about computer-aided education in the field of automatic control at ETH Zürich. Johansson et al [2] have developed an interactive design tool, which aims to design classical controllers like lead, lag or lead-lag compensator for use in automatic control education. Additionally, Azemi et al [3] have gathered a variety of programs that are used in teaching optimal control courses and prepared a toolbox for MATLAB for designing optimal controllers. The reader should note that all these examples including the COMES toolbox can be used to solve real engineering problems along with being educational aids. Sienel et al [4] and Sakabe et al [5] have created interactive MATLAB-based toolboxes for parameter space based robust control. Hyodo et al [6] have reported a MATLAB-based toolbox for parametric robust control. In reference [7], a robust control toolbox which combines Robust Control Toolbox, LMI and μ -Analysis and Synthesis Toolbox is given. Vivero and Castro [8] have introduced software for MATLAB to analyze and design multivariable control systems. Boyle et al [9] have designed an interactive design program for the frequency domain analysis and design of multivariable feedback systems in MATLAB. Campa et al [10] have created a new multivariable design program for linear systems analysis and robust control synthesis.

In this work, the Control of Mechatronic Systems (COMES) Toolbox has been developed. COMES is a user-friendly and user-extensible toolbox for designing control systems for mechatronic systems in the MATLAB environment. The

* Author of correspondence: guvencl@itu.edu.tr

COMES toolbox currently comprises of the four different widely used mechatronic system control methods which are: classical control, preview control, model regulator (also known as disturbance observer) control and repetitive control. These control systems can be used alone or can be used together as shown in the general block diagram of Figure 1. In the architecture of Figure 1, the model regulator controller works in an inner loop around the plant and forces the plant to behave like its nominal or desired model by rejecting external disturbances and being robust against model uncertainty. The classical controller is then added as a feedback controller which is designed for the nominal or desired plant. In the case of periodic reference or disturbance inputs, a repetitive controller is placed as an add-on feedback controller to reduce periodic error. A preview inverse filter is applied as a feedforward controller if the reference input is known a priori to improve tracking performance.

Classical control design is either based on parameter space robust control or the simpler design of lead, lag, PID type controllers using an analytical procedure for achieving a chosen gain crossover frequency with a desired phase margin and error constant. The synthesis technique behind the parameter space robust control approach is based on multi-objective mapping of Hurwitz stability, D -stability or the frequency domain specifications of weighted sensitivity or mixed sensitivity minimization or gain/phase margin bounds to a chosen controller parameter space. In preview control, three different kinds of discrete-time preview feedforward controllers such as zero phase error tracking (ZPET), precision tracking (PTC) and optimal precision tracking (OPTC) controllers can be designed using the COMES toolbox. Symbolic manipulation is used to determine the parameters of ZPET and PTC type feed-forward controllers. A constrained optimization problem with bandwidth and damping constraints is created and numerically solved using the evolutionary Big-Bang Big-Crunch optimization method for the design of OPTC type feed-forward control. To design both model regulator and repetitive control, a design method based on mapping a frequency domain mixed sensitivity bound into a chosen controller parameter space is used. The solution procedure results in colour filled graphical solution regions in the chosen controller parameter space. Hence, the user can focus on analyzing the graphical results without having to go through the underlying computations.

The first section of the paper presents the introduction and literature review. The general approach for control of mechatronic systems taken in the COMES tool is presented in Section 2. Sections 3 to 6 treat classical control, preview control, model regulator control and repetitive control, respectively. Moreover, the effectiveness of the use of this MATLAB-based toolbox is demonstrated in Sections 3-6 by carrying out some design and simulation studies for several position control applications available in the literature. The paper ends with conclusions presented in the last section.

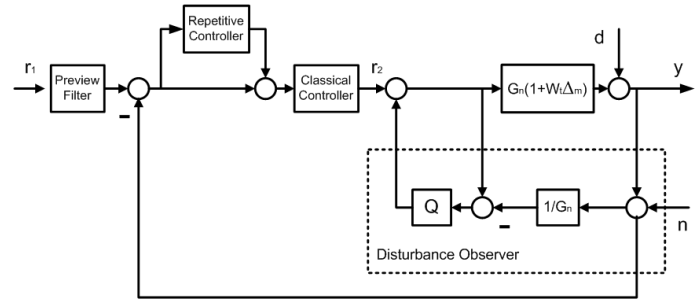


Figure 1. General control system structure.

2 ARCHITECTURE OF THE COMES TOOLBOX

COMES is an interactive MATLAB toolbox for designing advanced controllers systems for mechatronic systems driven by the following objectives: user friendliness, ease of code maintenance and code efficiency. The COMES toolbox currently comprises mainly of four different control strategies which are: Classical Control, Preview Control, Model Regulator Control and Repetitive Control. The toolbox also includes a general control methodology for parameter space based robust control that is used in some of the four main methods presented above. The current version of COMES supports parameter space based robust controller synthesis in terms of the objectives of: Hurwitz stability, D -stability, frequency-domain specifications of weighted sensitivity minimization and gain/phase margin specification. COMES also supports multi-objective design where these objectives are specified simultaneously.

The main window can be activated at the MATLAB prompt with the command "comes", and then a check is performed of the MATLAB version (that must be 6.5 or greater) and of the presence in the MATLAB path of the following toolboxes: Extended Symbolic Math Toolbox and Mapping Toolbox. If the MATLAB version is lower than 6.5, an error line will occur at the MATLAB prompt.

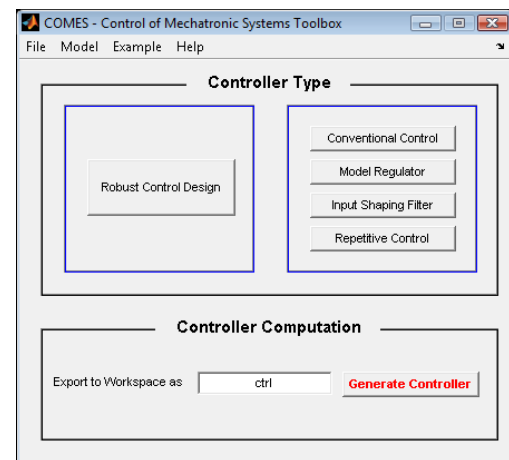


Figure 2. The main window of COMES toolbox.

A typical screenshot of the main GUI of the COMES toolbox is shown Figure 2. All synthesis and analysis procedures can be achieved by using the command buttons in the GUI accordingly. In "Controller Type" section, one of the four different control techniques mentioned above can be chosen by pressing buttons on the right hand side. Or, the button on the left hand side in Figure 2 can be pressed to carry out robust control design by using the parameter space approach.

When synthesizing a control system, the data and controller parameters, which are calculated by means of the COMES toolbox, are automatically sent to the MATLAB workspace as a structure named "COMES_wrkspc". The desired data such as controller parameters and parameter space plots can be chosen from this structure.

3 CLASSICAL CONTROL

Classical (also called *conventional* in this paper and in COMES) control techniques work best for single-input-single-output (SISO), linear time-invariant (LTI) systems where the required performance specifications are given in the time and/or frequency-domain. In spite of the presence of a large number of advanced control techniques in the literature, classical control methods are widely used in the control of mechatronic systems because they can easily be implemented as real-time systems at relatively low cost.

Trial and error procedures are used extensively in designing conventional controllers like lead, lag or lead-lag compensator in the frequency-domain [13-18]. In contrast, analytical frequency domain methods are used for tuning the parameters of classical controllers like lead, lag, lead-lag and PID controllers in COMES.

Analytical solution procedure for root-locus based design of classical control systems was reported in the references by Ross, Warren, Thaler and Wakeland [19-21]. Wakeland presented an analytical solution technique to eliminate the trial and error procedure in the design of a lead-lag compensator [22]. Mitchell improved this methodology for the lead and lag compensators [23]. The analytical solution technique in the frequency domain mentioned above is based upon solution for a specified phase margin. A similar approach where the appropriate error constant, gain crossover frequency and phase margin are specified is used here.

3.1 Analytical Design in Frequency Domain:

The analytical phase margin based design is outlined for the case of a phase lead compensator in this sub-section.

Step1: Evaluate the phase lead compensator gain $K_c\alpha$ so that the desired error constant K_{error} (position, velocity, acceleration) is obtained. Then, the compensator transfer function is rewritten as

$$C(s) = K_c\alpha \frac{\tau s + 1}{\alpha \tau s + 1} = K_c\alpha C_p(s) \quad (1)$$

$$C_p(s) = \frac{\tau s + 1}{\alpha \tau s + 1} \quad (2)$$

The rest of the procedure involves designing C_p for the desired phase margin at the desired gain crossover frequency. The designed $C_p(s)$ should satisfy

$$\left| C_p(j\omega_{gc}) \left[K_c\alpha G(j\omega_{gc}) \right] \right| = 1 \quad (3)$$

$$\theta = \angle \left(C_p(j\omega_{gc}) \right) = \pi + \phi_m + \tau_d \omega - \angle \left(G(j\omega_{gc}) \right) \quad (4)$$

where G is the plant, ϕ_m is the desired phase margin and ω_{gc} is the gain crossover frequency. The gain margin obtained should be checked at the end of the design procedure. Equations (3) and (4) are the angle and magnitude equations, respectively. When the desired phase margin ϕ_m and the desired gain crossover frequency ω_{gc} are selected, only the two unknowns α and τ remain in the two equations above. It is possible to solve for these two unknowns as

$$\frac{1}{\alpha \tau} = \frac{\sin \theta}{\cos \theta - K_c\alpha \left| G_p(j\omega_{gc}) H(j\omega_{gc}) \right|} \omega_{gc} \quad (5)$$

$$\frac{1}{\tau} = \frac{\sin \theta}{\frac{1}{K_c\alpha \left| G_p(j\omega_{gc}) H(j\omega_{gc}) \right|} - \cos \theta} \omega_{gc} \quad (6)$$

The derivation of these two equations is skipped here (given in reference [96]). There are some constraints that must be satisfied for obtaining meaningful (real and positive) solutions of (5) and (6).

Step2: Generate the Bode diagram of the open loop control system ($K_c\alpha G(s)$) and locate the existing gain crossover frequency ω_{gc} . Choose the new gain crossover frequency ω_{gc} subject to $K_c\alpha G(s)|_{s=j\omega}$ having magnitude lower than 0dB.

Step3: Evaluate the angle θ using

$$\theta = \pi + \phi_m - \angle \left(G(j\omega_{gc}) \right) \quad (7)$$

Step4: Evaluate $1/\tau$ and $1/(\alpha\tau)$ using equations (5) and (6).

Step5: Draw the Bode diagram of compensated system $C(s)G(s)$. Evaluate the phase and gain margins.

3.2 Parameter Space Approach:

The method presented in this sub-section relies on mapping Hurwitz stability, D -stability and frequency domain constraints on closed-loop transfer functions like nominal performance, robust stability and robust performance and gain/phase margin bounds to the parameter space of chosen controller parameters. A fixed controller structure is used (see reference [22] for example). References focusing on mapping frequency domain specifications into parameter space can be found in [23-31].

3.2.1 Hurwitz Stability Design:

The family of polynomials $P(s, Q)$ is robustly stable, if and only if,

- there exists a stable polynomial $p(s, q) \in P(s, Q)$.
- $j\omega \notin \text{Roots}[P(s, Q)]$ for $\forall \omega \geq 0$.

If one plots the curves in the parameter plane where $j\omega \in \text{Roots}[P(s, Q)]$ holds, it is obviously understood that the parameters have to cross this boundary, for the roots of the characteristic polynomial to cross the imaginary axis. If all the roots of the polynomial were on the left half plane then basically this cross would destabilize the system. Hence, this boundary can be called the stability boundary. However, the second boundary crossing condition will be used in a different manner while synthesizing the controller. Notice that if the value of the polynomial has zero value for $\exists \omega \geq 0$ then it is basically has a root on the imaginary axis exactly at that frequency. If

$$p(j\omega, q) = 0 \quad (8)$$

holds for some $q \in Q$ then this polynomial family is on the stability margin. The task in the controller design is to plot the q values on the parameter space such that (8) holds. In this manner the stability boundaries can be observed upon variations of $q \in Q$. Choosing two parameters to be varying and evaluating (8) would yield,

$$\begin{aligned} p(j\omega, q) &= (a_0(q) - a_2(q)\omega^2 + a_4(q)\omega^4 - \dots) \\ &+ j\omega(a_1(q) - a_3(q)\omega^2 + a_5(q)\omega^4 - \dots) = 0 \end{aligned} \quad (9)$$

Equation (9) can be broken up into a real and an imaginary part equation as

$$\begin{aligned} a_0(q) - a_2(q)\omega^2 + a_4(q)\omega^4 - \dots &= 0 \\ a_1(q) - a_3(q)\omega^2 + a_5(q)\omega^4 - \dots &= 0 \end{aligned} \quad (10)$$

Now, let us fix all the uncertain parameters except two, which may be uncertain parameters of the plant or the controller,

$$a_0(q_1, q_2) - a_2(q_1, q_2)\omega^2 + a_4(q_1, q_2)\omega^4 - \dots = 0 \quad (11)$$

$$\omega(a_1(q_1, q_2) - a_3(q_1, q_2)\omega^2 + a_5(q_1, q_2)\omega^4 - \dots) = 0 \quad (12)$$

The first approach should be to eliminate ω from the above equations and then plot the solution in the q_1 - q_2 plane. However, note that this would then result in solutions for complex values of ω [22]. Instead of this elimination, the frequency ω is chosen as a parameter being varied in the interval $0 \leq \omega \leq \infty$. At each frequency ω , the parameters q_1 and q_2 are solved from the equation set (11), and the result is plotted in the parameter space of q_2 versus q_1 . If the grid over the frequency ω is dense enough, then the resulting curve will be a candidate for the stability boundary. By leaving ω in the equations one can restrict its values to non-negative real values, thus avoiding fictitious boundaries where ω takes complex values.

Roots of the uncertain polynomial will cross the imaginary axis through $\omega=0$, $\omega=\infty$ or $0 < \omega < \infty$. Note that for $\omega=0$ equation (12) drops and the two parameters in consideration become dependent. Then the solution becomes a single line in the parameter space. The equation of this line can be obtained from (11) explicitly. This line which provides the boundary over which a crossing occurs through the origin is called the “real root boundary” (RRB). This condition is equivalent to $a_0=0$.

The crossing through $\omega=\infty$ is possible when the polynomial drops degree, which can be given as $a_n=0$. The equation is again explicit in terms of the uncertain parameters, and it forms a line in the two dimensional parameter space. This line is called the “infinite root boundary” (IRB). Finally the solution of (11) and (12) for $0 < \omega < \infty$ gives curves in the two dimensional parameter space and these curves are called the “complex root boundary” (CRB).

3.2.2 D-stability Design:

The abovementioned Hurwitz stability parameter space region computation procedure can be extended to relative stability called D -stability. The roots of the characteristic polynomial of the closed-loop system should be located inside of the D -stability region in the complex plane as shown in Figure 3 if this system is D -stable.

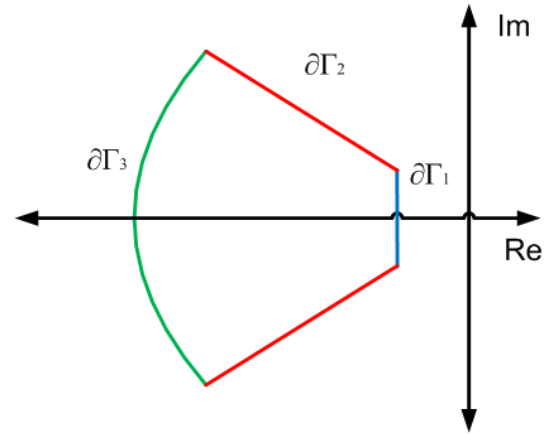


Figure 3. D-stability region

The D -stability boundary ($\partial\Gamma$) can be described mathematically by:

$$\partial\Gamma = \{s | s = \sigma(a) + ja\alpha(a), a \in [a^-, a^+]\} \quad (13)$$

The D -stability boundary has to be mapped to the parameter space to obtain $Q_{\Gamma\text{-stable}}$. For this purpose, we need to express $\partial\Gamma$ in a more convenient way. For the D -stable region shown in Figure 3.1 the D -stability boundary can be expressed as

$$\partial\Gamma = \partial\Gamma_1 + \partial\Gamma_2 + \partial\Gamma_3 \quad (14)$$

The boundary $\partial\Gamma_1$ in Figure 3 can be mapped into the parameter space by substituting $(s - \sigma)$ for s in (9) so as to shift the stability boundary to $\partial\Gamma_1$ in the complex plane. After that, solving for the controller parameters in (11) and (12) in the same manner as before and plotting the result in the chosen controller parameter plane leads to the ∂_1 boundary in the parameter space. Notice that no infinite root boundary (IRB) exists because s is never equal to infinity in the D -shaped region shown in Figure 3. In order to map the boundary $\partial\Gamma_2$ to the chosen parameter plane, we will use $re^{j\theta}$ for s in equation (9) and parameterize r in $a_0=0$ to obtain the complex root boundary (CRB) of $\partial\Gamma_1$ after solving for the chosen controller parameters. No singular solution exists because r is never equal

to zero or infinity. In addition, mapping the boundary $\partial\Gamma_3$ to the chosen parameter plane can be carried out by substituting s with $Re^{j\theta}$ where R is a constant. The real root boundaries (RRB) $\partial\Gamma_1$, $\partial\Gamma_3$ and complex root boundaries (CRB) $\partial\Gamma_1$, $\partial\Gamma_2$, $\partial\Gamma_3$ are obtained symbolically in terms of chosen controller parameters.

3.2.3 Phase/Gain Margin Design:

The constant phase margin boundary can be plotted in a chosen controller parameter space. The constant phase margin boundary satisfies the following equation

$$L(j\omega) := C(j\omega)G(j\omega) = e^{j(m_\phi - \pi)} \quad (15)$$

where m_ϕ is the phase margin bound. Assume that the controller is given by $C(s) = N_C(s)/D_C(s)$ with

$$\begin{aligned} N_C(j\omega) &= N_{C,R}(j\omega) + jN_{C,I}(j\omega) \\ D_C(j\omega) &= D_{C,R}(j\omega) + jD_{C,I}(j\omega) \end{aligned} \quad (16)$$

and the plant $G(s) = N(s)/D(s)$ is given by

$$\begin{aligned} N(j\omega) &= N_R(j\omega) + jN_I(j\omega) \\ D(j\omega) &= D_R(j\omega) + jD_I(j\omega) \end{aligned} \quad (17)$$

The real and imaginary parts of $L(j\omega)$ can be expressed as

$$\begin{aligned} \text{Re}[L(j\omega)] &= \text{Re}\left[\frac{N_{C,R} + jN_{C,I}}{D_{C,R} + jD_{C,I}} \frac{N_R + jN_I}{D_R + jD_I}\right] = -\cos(m_\phi) \\ \text{Im}[L(j\omega)] &= \text{Im}\left[\frac{N_{C,R} + jN_{C,I}}{D_{C,R} + jD_{C,I}} \frac{N_R + jN_I}{D_R + jD_I}\right] = -\sin(m_\phi) \end{aligned} \quad (18)$$

Using the two equations (18), the chosen two controller parameters can be solved for symbolically.

Notice that the symbolic solutions might be too long in size for higher order choices of these filters, necessitating a numerical solution. The constant gain margin region parameterization is also possible as it is obtained in a similar manner.

3.2.4 Design by Mapping Frequency domain bounds:

The aim of this section is to map the frequency domain criteria of robust control to parameter space. The mixed sensitivity problem will be considered in the analysis. Similar to the parameter space approach given in [33], the parameter space design is based on satisfying the mixed sensitivity requirement

$$\|W_S S + W_T T\|_\infty < 1 \quad (19)$$

or equivalently satisfying

$$|W_S S| + |W_T T| < 1 \quad \text{for } \forall \omega \quad (20)$$

where S and T are the sensitivity and complementary sensitivity transfer functions and W_S and W_T are the corresponding weights. Under the limit condition, this requirement can be presented as

$$|W_S| + |W_T L| = |1 + L| \quad \text{for } \forall \omega \quad (21)$$

which is called the point condition at each frequency. L in equation (21) is the loop gain. In order to obtain the region which satisfies expression (20) for all frequencies in the

parameter space, equation (21) must be solved frequency at a time. The intersection of the regions for every calculated frequency leads to the overall solution region. The point condition is graphically illustrated in Figure 4.

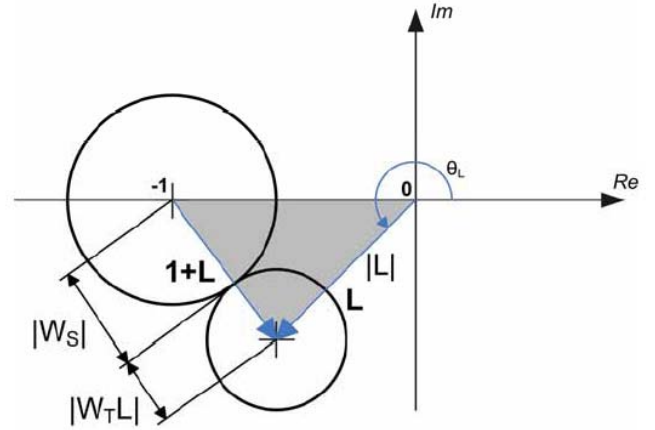


Figure 4. Point condition for the mixed sensitivity.

By applying the cosine rule to the shaded triangle in Figure 4 and solving the quadratic equation obtained for $|L|$ results in,

$$|L(j\omega)| = \frac{(-\cos \theta_L + |W_S(\omega)| |W_T(\omega)|) \pm \sqrt{\Delta_M(\omega)}}{1 - |W_T(\omega)|^2} \quad (22)$$

where

$$\Delta = \cos^2 \theta_L + |W_S|^2 + |W_T|^2 - 2|W_S||W_T|\cos \theta_L - 1 \quad (23)$$

The solution procedure is to sweep angle θ_L from 0 to 2π radians and to solve for $|L|$ at each value of θ_L for which a solution exists. Then, all possible values of $L = |L|e^{j\theta_L}$ at the chosen frequency ω are obtained. Each value of L satisfies

$$L = CG = (C_R + jC_I)G \quad (24)$$

where C is the controller. The reader can be referred to [24] and [34] and the references therein for details of the general method of mapping frequency domain bounds to parameter space for standard feedback control architecture.

3.3 Example:

Consider the system analyzed in [22]. The open-loop transfer function is given by

$$G(s) = \frac{1}{s(1+0.2s)(1+0.45s)} \quad (25)$$

Solution I: It is desired to design a compensator for the plant in (25) so that the static velocity error constant K_v is 4 sec^{-1} , the phase margin is at least 55° and gain crossover frequency is 4.25 rad/sec . The Conventional Controller Design module of the COMES toolbox is used to design a lead compensator that satisfies the desired design specifications.

In Figure 5, the general structure of the Conventional Controller Design GUI of COMES based on MATLAB is demonstrated. On the right side of Figure 5, the Bode magnitude and phase plots can be seen. In these plots, the blue curve denotes the uncompensated system and the red curves denote the compensated system. The type of controller which will be designed can be chosen from the "Controller Type" option in the menu bar. According to the chosen controller type, the corresponding sections seen on the left hand side of Figure 5 are activated.

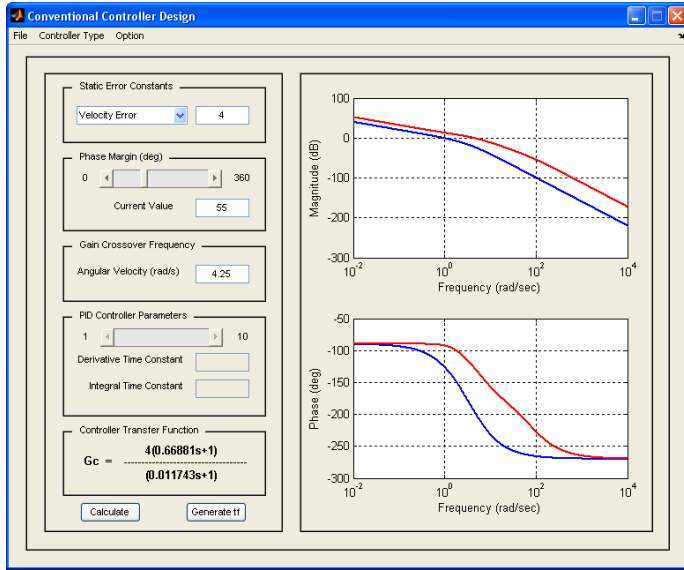


Figure 5. Lead compensator design with the conventional control part of COMES toolbox.

Solution II: Using the parameter space methodology, a robust PD controller is designed for the plant given in (25). On the right side of Figure 6, the D -stability region with the constraints $\sigma=1$, $\theta=120^\circ$ and $R=7.5$ is seen. Additionally, the pole locations of the closed-loop control system are demonstrated for the chosen PD controller parameters on the left side of Figure 6 with cross marks. In Figure 7, the phase margin design is given for the chosen controller parameters. The parameter space calculation is done for the desired minimum phase margin values varying between 15° and 90° . By utilizing the Robust Control module of the COMES toolbox, the PD controller satisfying the desired design specifications was designed successfully.

4 PREVIEW CONTROL

The goal of the preview (reference feedforward tracking) control is to obtain a low-pass filter of desired tracking bandwidth between the input and output to reduce tracking error below what is achievable with feedback alone. A two degree of freedom (2 DOF) controller architecture is utilized in order to achieve this purpose by cascading the closed-loop control system, already under feedback control, with its

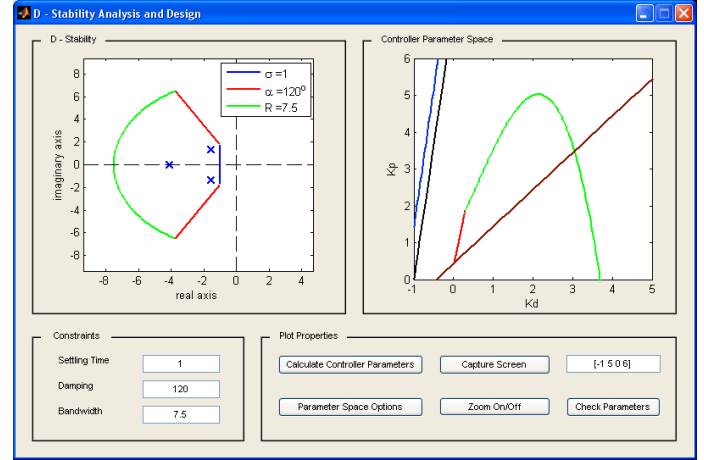


Figure 6. D -stability analysis and design part of COMES toolbox.

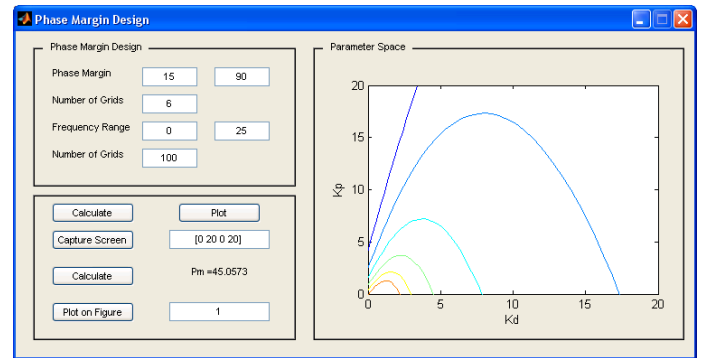


Figure 7. Phase margin design in COMES toolbox.

approximate inverse, as show in Figure 1. Seeking an exact inverse based on pole-zero cancellation to achieve perfect compensation of the plant or closed-loop system is the ideal goal. This is not possible since nonminimum phase (NMP) zeros, if they exist, cannot be inverted directly. NMP zeros are common in models of process control systems with transport lag [13] and flexible structure [36]. Exact inversion is not a good idea even if the system consists of only minimum phase zeros because of the presence of model uncertainties at high frequencies. Application of the approximate inverse should result in low-pass filter characteristics between system's input and output.

There are several methods in the literature for designing approximate inverse filters for discrete-time systems with NMP zeros. The earliest method in the literature is the zero phase error tracking (ZPET) control of Tomizuka [37], where the phase error due to the NMP zeros is eliminated for achieving zero phase error trajectory tracking. However, ZPET filter cannot eliminate the gain error due to the NMP zeros. For this purpose, this gain error can be compensated by utilizing E-filter [38], precision tracking control (PTC) [39] or optimal precision tracking control (OPTC) [40]. Extended precision tracking

control (EPTC) [41] is able to tackle discrete-time systems with complex NMP zeros as well as real ones. Furthermore, the designers have more freedom while using the EPTC method because both the desired tracking bandwidth and flat low frequency gain characteristics can be obtained in comparison to just one of them achieved in the PTC method. In the truncated series approximation (TSA) method of Gross et al [42], polynomial long division is utilized to obtain a non-zero phase solution.

4.1 Preview Control Structure:

There preview control methods currently implemented in COMES are the zero phase error, precision tracking and optimal precision tracking methods.

4.1.1 Zero Phase Error Tracking (ZPET) Control:

The earliest method of designing preview control system based on reference feedforward controllers is the ZPET scheme of Tomizuka [37], where the phase error due to the NMP zeros are eliminated in order to achieve zero phase error trajectory tracking.

Let the transfer function of the closed-loop control system in discrete time be given by

$$G_{cl}(z) = \frac{n_{mp}(z)n_{nmp}(z)}{d(z)} \quad (26)$$

where $n_{mp}(z)$ and $n_{nmp}(z)$ are the minimum and non-minimum phase parts, respectively, of the numerator. The non-minimum phase part of the numerator can be factored into

$$n_{nmp}(z) = \prod_{k=1}^m (z - z_k) \quad (27)$$

$z_k \in \mathbb{C}, |z_k| \geq 1$

where \mathbb{C} denotes complex numbers and z_k are the m non-minimum phase zeros of the closed loop system. Note that complex conjugation of factors of the form $z - z_k$ ($z_k \in \mathbb{C}$) over the unit circle ($z = e^{j\theta}$) amounts to

$$\overline{(z - z_k)} \Big|_{z=e^{j\theta}} = (z^{-1} - \bar{z}_k) \Big|_{z=e^{j\theta}} \quad (28)$$

The ZPET approximate inverse of $G_{cl}(z)$ is given by

$$\tilde{G}_{ZPET}^{-1}(z) = \frac{d(z)}{n_{mp}(z)} \prod_{k=1}^m \frac{(z^{-1} - \bar{z}_k)}{(1 - z_k)(1 - \bar{z}_k)} \quad (29)$$

The first part of equation (29) is the invertible part of $G_{cl}(z)$. The remaining part of equation (29) is there so that the compensated system $\tilde{G}_{ZPET}^{-1}(z)G_{cl}(z)$ has zero phase angle at all frequencies and unity d.c. gain. Whatever can be inverted in $G_{cl}(z)$ has been inverted and the remaining nonminimum phase part has been multiplied by its complex conjugate in the frequency domain. The $(1 - z_k)$ type terms in the denominator of equation (29) are introduced to make the d.c. gain of the feedforward compensated system equal to unity.

The transfer function of the ZPET feedforward compensated system becomes

$$\tilde{G}_{ZPET}^{-1}(z)G_{cl}(z) = \prod_{k=1}^m \frac{(z - z_k)(z^{-1} - \bar{z}_k)}{(1 - z_k)(1 - \bar{z}_k)} \quad (30)$$

4.1.2 Precision Tracking Control (PTC):

The ZPET approach might increase the gain errors while the phase errors are cancelled. Therefore, the desired tracking control characteristics can be obtained only within a relatively small bandwidth. For this reason, the zero phase error of the ZPET method should be combined with a gain error compensation method. To achieve this purpose, the PTC (Precision Tracking Control) method adds gain error compensating zeros while preserving zero phase error characteristics [39].

In the PTC method, terms involving real nonminimum phase zeros are separated into two different categories as type I and type II based on whether their amplitude Bode plots rise or fall with respect to frequency. Gain error due to type I NMP zeros can be compensated by adding appropriate type II NMP zeros to the feedforward compensator and vice versa. The PTC feedforward compensator is given by

$$\tilde{G}_{PTC}^{-1}(z) = \frac{d(z)}{n_{mp}(z)} \prod_{k=1}^m \frac{(z^{-1} - \bar{z}_k)}{(1 - z_k)(1 - \bar{z}_k)} \frac{(z - z_k^*)(z^{-1} - \bar{z}_k^*)}{(1 - z_k^*)(1 - \bar{z}_k^*)} \quad (31)$$

where $z_k^* \in \mathbb{C}$ indicates the gain compensating zero corresponding to the NMP zero z_k . The PTC feedforward compensator given in equation (31) adds a gain compensating zero expression multiplied by its complex conjugate on the unit circle for preserving zero phase between input and output. The transfer function of the feedforward compensated system becomes

$$\tilde{G}_{PTC}^{-1}(z)G_{cl}(z) = \prod_{k=1}^m \frac{(z - z_k)(z^{-1} - \bar{z}_k)(z - z_k^*)(z^{-1} - \bar{z}_k^*)}{(1 - z_k)(1 - \bar{z}_k)(1 - z_k^*)(1 - \bar{z}_k^*)} \quad (32)$$

The gain compensating zeros are determined by solving

$$\left| \tilde{G}_{PTC}^{-1}(e^{j\theta})G_{cl}(e^{j\theta}) \right|_{\theta=\theta^*} = 1 \quad (33)$$

and equation (31) for z_k^* . By utilizing the PTC method, the system tracking bandwidth can be improved, thus improving the tracking accuracy. However, it should also be kept in mind that PTC is not an optimal method and there are situations where a specified desired bandwidth value cannot be achieved..

4.1.3 Optimal Precision Tracking Control (OPTC):

In this section, the nonminimum phase part of the numerator is factored into

$$n_{nmp}(z) = \prod_{k=1}^{m_r} (z - z_k) \prod_{l=1}^{m_c} (z - z_l)(z - \bar{z}_l) \quad (34)$$

and has m_r real and m_c complex conjugate pairs of NMP zeros. Hence, $n_{nmp}(z)$ in expression (34) has a total of $m_r + 2m_c$ NMP zeros.

The OPTC preview feedforward compensator is given by

$$\tilde{G}_{OPTC}^{-1}(z) = \left[\frac{d(z)}{n_{mp}(z)} \right] \left[\prod_{k=1}^{m_r} \frac{(z^{-1} - \bar{z}_k)}{(1 - z_k)^2} \prod_{l=1}^{m_c} \frac{(z^{-1} - z_l)(z^{-1} - \bar{z}_l)}{(1 - z_k^*)(1 - \bar{z}_k^*)} \right] \left[\prod_{r=1}^{m_r} \frac{(z - z_r)(z^{-1} - z_r)}{(1 - z_r)^2} \right] \left[\prod_{c=1}^{m_c} \frac{(z - z_c)(z^{-1} - \bar{z}_c)(z - \bar{z}_c)(z^{-1} - z_c)}{(1 - z_c)^2(1 - \bar{z}_c)^2} \right] \quad (35)$$

where $z_r \in \mathbb{R}$ and $z_c \in \mathbb{C}$. The first expression of equation (35) is the invertible part of $G_{cl}(z)$ in equation (26). The second expression of equation (35) is the zero phase compensation of $n_{nmp}(z)$ in Equation (34). The last two expressions are used for gain error compensation with m_r real and m_c complex conjugate pairs of gain compensation zeros while preserving the zero phase angle property. The compensated system $\tilde{G}_{ZPET}^{-1}(z)G_{cl}(z)$ has by construction zero phase at all frequencies and the gain compensation zeros are determined optimally by solving the optimization problem

$$\min_{\substack{z_r \in \mathbb{R}; r=1,2,\dots,m_r \\ z_c \in \mathbb{C}; c=1,2,\dots,m_c}} \int_0^\pi |W(\theta)(1 - \tilde{G}_{PTC}^{-1}(e^{j\theta})G_{fb}(e^{j\theta}))|^2 d\theta \quad (36)$$

$W(\theta)$ in expression (36) is a weighting function that is usually chosen as

$$W(\theta) = \begin{cases} 1, & \theta \leq \theta^* \\ 0, & \theta > \theta^* \end{cases} \quad (37)$$

where θ^* is the desired bandwidth of preview feedforward compensation. Moreover, the weight can be alternatively chosen in order to minimize the tracking error for an input signal if the desired input trajectory is known in advance. The formulation give in equation (36) works well for both real and complex conjugate NMP zeros. However, there could be some problems when the complex conjugate NMP zeros are close to the imaginary axis or unit circle.

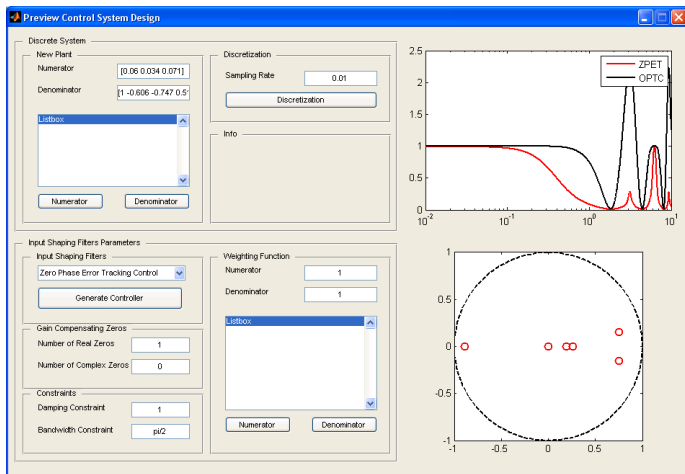


Figure 8. A screenshot of preview control part of COMES toolbox.

4.2 Example:

The closed-loop position control system of a hydraulic linear actuating system which is used for tool positioning in noncircular machining in [47] is chosen for the simulation study since its model includes a complex conjugate NMP zero pair. The discrete time, reduced order model of closed-loop system is given by

$$G(z) = \frac{0.06z^2 + 0.034z + 0.071}{z^7 - 0.606z^6 - 0.747z^5 + 0.519z^4} \quad (38)$$

The complex NMP zeros are $z_1, \bar{z}_1 = -0.2833 \pm j1.0503$. This pair of complex conjugate NMP zero is close to the imaginary axis and the unit circle. For this reason, they are hard to compensate. In addition, the gain plot has a valley close to $\theta = \pi/2$ rad and then it rises to about unity at $\theta = \pi$ rad. To compensate for this gain characteristic, the compensating zeros must be added for introducing sufficient gain attenuation at high frequencies. However, the optimization formulation given in (36) might create some problems for this kind of hard to compensate complex conjugate NMP zero pairs. For this purpose, the weighting function $W(\theta)$ is selected to have large gain at high frequencies above θ^* and is chosen in this case study as $3.61/|e^{j\theta} + 0.9|^2$ to provide large weight at high frequencies.

The OPTC calculations, successively, with one real, two real and one complex conjugate gain compensating zero pair led to the best result obtained by the two real zeros case ($m_r=2$ and $m_c=0$). The two real gain compensating zeros are $z_1=0.0867$ and $z_2=0.2874$. The magnitude frequency response plots seen in the COMES screenshot in Figure 8 show the comparison between the gain compensation ability of two input shaping filters: ZPET and OPTC.

5 MODEL REGULATOR CONTROL

The model regulator (disturbance observer) is a particular method of designing a two degree-of-freedom (2 DOF) control architecture in order to achieve insensitivity against modelling errors due to model order reduction, linearization and excellent disturbance rejection [48-49]. It has been successfully applied to many application areas including motion control applications including high speed direct drive positioning [50], friction compensation [51] and vehicle steering control [52-53]. The augmentation of a plant with the model regulator forces it to behave just like its nominal (or desired) model within the bandwidth of model regulator, called the bandwidth of the model regulation. The model regulation (see inner feedback loop in Fig. 1) can be achieved by means of comparing the actual input to the plant with the input that should have been applied to obtain the measured output based on the nominal (or desired) knowledge of the plant. The difference is then passed through a positive feedback loop. Disturbance rejection and

model regulation are the two very important features of a disturbance observer.

The disturbance observer introduces stability and stability robustness problems due to the use of positive feedback. Use of unstructured model uncertainty and low-pass filtering of the disturbance observer output is a very practical manner to avoid stability robustness problems at high frequencies due to the presence of unmodeled dynamics.

5.1 Model Regulator Structure:

The loop gain of the disturbance observer compensated plant in Fig. 1 is given by

$$L = \frac{GQ}{G_n(1-Q)} \quad (39)$$

with the model regulation, disturbance rejection, and sensor noise rejection transfer functions given by:

$$\frac{y}{r} = \frac{G_n G}{G_n(1-Q) + GQ} \quad (40)$$

$$\frac{y}{d} = \frac{G_d}{1+L} \equiv G_d S = \frac{G_n(1-Q)G_d}{G_n(1-Q) + GQ} \quad (41)$$

$$\frac{y}{n} = \frac{-L}{1+L} \equiv -T = \frac{-GQ}{G_n(1-Q) + GQ} \quad (42)$$

In (41) and (42), S and T are the sensitivity and complementary sensitivity, functions, respectively. Q is chosen as a low pass filter with unity d.c. gain. This choice of Q results in $y/r \rightarrow G_n$ which is the desired steering dynamics, $y/d \rightarrow 0$ (disturbance rejection) at low frequencies where $Q \rightarrow 1$. At higher frequencies where there may be considerable sensor noise, $y/n \rightarrow 0$ (sensor noise rejection) will be achieved as $Q \rightarrow 0$. This choice of $Q \rightarrow 0$ at higher frequencies is also necessary for the robustness of stability. Then, the input-output behaviour of the controlled system including its steady-state behaviour will be the same as those of the nominal (or desired) model G_n up to the bandwidth of the low pass filter Q (control system regulation along with good disturbance rejection). A screenshot of the model regulator design part of the COMES toolbox is shown in Fig. 9.

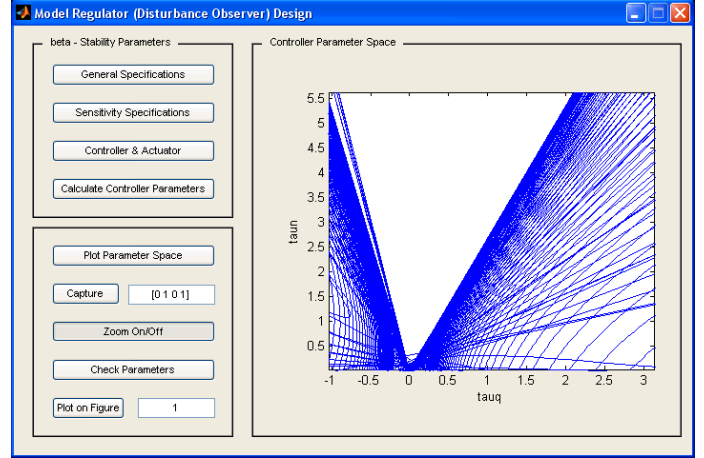


Figure 9. A screenshot of model regulator control part of COMES toolbox.

6 REPETITIVE CONTROL

Repetitive controllers are used to accurately track periodic reference signals or to reject periodic disturbances with known period by introducing a highly frequency selective gain through a positive feedback loop which contains a time delay element as it is a generator of periodic signals. The delay time is equal to the known period of the repetitive reference (or disturbance) signal. Significant improvement in the tracking accuracy or disturbance rejection characteristics of systems subject to periodic exogenous signals can be achieved using repetitive control. The idea of repetitive control was first created by Inoue et al [57] to replace conventional motion control techniques in the control of a proton synchrotron magnet power supply. Until recently, it has been widely utilized in many application areas including control of hard disc drives [58], control of optical disc drives [59], control of noncircular tuning [47], trajectory control of industrial robot arms [60, 61], motor speed control [62], high precision rotational control [63], control of material testing machine [64], control of cold rolling process [65], suppression of torque vibration in motors [66], reduction of waveform distortion in PWM inverter or UPS [67-69] and accurate position control of piezoelectric actuators [70, 71].

6.1 Repetitive Control Structure:

Consider the add-on repetitive control structure shown in the upper part of Figure 1. G_n is the nominal model of the plant, Δ_m is the normalized unstructured multiplicative model uncertainty, W_T is the multiplicative uncertainty weighting function and τ_d is the period of the periodic exogenous signal. $q(s)$ and $b(s)$ are filters used for tuning the repetitive controller. Repetitive control systems can track periodic signals very accurately and can reject periodic disturbances very satisfactorily. This is due to the fact that the positive feedback loop within the repetitive controller in Fig. 1 is a generator of periodic signals with period τ_d for $q(s)=1$. A low pass filter with

unity d.c. gain is used for $q(s)$ for robustness of stability [18, 25].

The repetitive controller design involves the design of the two filters $q(s)$ and $b(s)$ seen within the repetitive control part of Figure 1. In the frequency domain, the ideal low-pass filter $q(j\omega)$ would be 1 in the frequency range of interest and zero at higher frequencies. This is not possible and $q(j\omega)$ will have negative phase angle which will make $q(j\omega)$ differ from 1, resulting in reduced accuracy. So as to improve the accuracy of the repetitive controller, a small time advance is customarily incorporated into $q(s)$ to cancel out the negative phase of its low-pass filter part within its bandwidth. This small time advance can easily be absorbed by the much larger time delay τ_d corresponding to the period of the exogenous input signal and does not constitute an implementation problem.

The main objective of the usage of the dynamic compensator $b(s)$ is improving the relative stability, the transition response and the steady state accuracy in combination with the low-pass filter $q(s)$. Consider the function of frequency given by

$$R(\omega) = \left| q(j\omega) \left[1 - b(j\omega) \frac{G(j\omega)}{1+G(j\omega)} \right] \right| \quad (43)$$

$R(\omega) < 1$ is a sufficient condition for stability and making $R(\omega)$ as small as possible is a design aim as $R(\omega)$ is also a measure of relative stability. Accordingly, the compensator $b(s)$ is designed to approximately invert $G/(1+G)$ within the bandwidth of $q(s)$ in an effort to minimize $R(\omega)$. The dynamic compensator $b(s)$ can be selected as only a small time advance or time advance multiplied by a low-pass filter in order to minimize $R(\omega)$. In order to make $R(\omega)$ as small as possible, the time advance in the filter $b(s)$ is chosen to cancel out the negative phase of $G/(1+G)$. This small time advance can easily be absorbed by the much larger time delay τ_d corresponding to the period of the exogenous input signal and does not constitute an implementation problem.

The $q(s)$ and $b(s)$ filters are thus expressed as

$$q(s) = q_p(s) e^{\tau_q s} \quad (44)$$

$$b(s) = b_p(s) e^{\tau_b s} \quad (45)$$

The time advances τ_q and τ_b are chosen to decrease the magnitude of $R(\omega)$ given in Eq. (43). Then, the design focuses on pairs of chosen parameters in $q_p(s)$ or $b_p(s)$ to satisfy a frequency domain bound on the robust performance criterion. Let L denote the loop gain of the repetitive control system, and S and T denote its sensitivity and complementary sensitivity transfer functions. The parameter space repetitive controller design used in COMES aims at choosing parameter space regions of a chosen pair of parameters in $b_p(s)$ and/or $q_p(s)$ where the condition

$$|W_s S| + |W_T T| < 1 \quad \text{for } \forall \omega \quad (46)$$

which is similar to satisfying the robust performance requirement $\|W_s S\| + \|W_T T\|_\infty < 1$ where W_s and W_T are the sensitivity and complementary sensitivity function weights.

The loop gain of the repetitive controlled system (see Figure 1) is given by

$$L = G_n \left(1 + \frac{q_p}{1 - q_p e^{(-\tau_d + \tau_q + \tau_b)s}} b_p e^{(-\tau_d + \tau_q + \tau_b)s} \right) \quad (47)$$

Condition (46) is equivalent to

$$\begin{aligned} |W_s(\omega) S(j\omega)| + |W_T(\omega) T(j\omega)| \\ = \left| \frac{W_s(\omega)}{1 + L(j\omega)} \right| + \left| \frac{W_T(\omega) L(j\omega)}{1 + L(j\omega)} \right| < 1 \quad \text{for } \forall \omega \end{aligned} \quad (48)$$

or equivalently

$$|W_s(\omega)| + |W_T(\omega) L(j\omega)| < |1 + L(j\omega)| \quad \text{for } \forall \omega \quad (49)$$

6.2 Example:

In this part of the paper, the high speed atomic force microscope (AFM) scanner which is designed and modeled in [31] is utilized as a numerical example to explain the methodology of the multi-objective parameter space approach for SISO repetitive controller design programmed in COMES. The second order and fourth order mathematical models of this high speed AFM scanner are given in [31]. In this example, the fourth order model is used because it includes the first mode of the piezoelectric stack in the vertical direction. The transfer function of the AFM scanner is given by

$$G(s) = \frac{K(s^2 + 2\zeta_2\omega_2s + \omega_2^2)}{(s^2 + 2\zeta_1\omega_1s + \omega_1^2)(s^2 + 2\zeta_3\omega_3s + \omega_3^2)} [nm/V] \quad (50)$$

Where $K = 1 \times 10^{12} nm/V$ includes the power amplifier and sensor gain. The system seen in (50) has two resonant frequencies and one anti-resonant frequency. The numerical values of these frequencies are given as $f_1 = 40.9 kHz$, $f_2 = 41.6 kHz$ and $f_3 = 120 kHz$. The numerical values of the relative damping coefficients are given as $\zeta_1 = 0.016$, $\zeta_2 = 0.016$ and $\zeta_3 = 0.17$. The dynamic compensator $b(s)$ is chosen as a pure time advance as

$$b(s) = b_p(s) e^{\tau_b s} = e^{3 \times 10^{-6} s} \quad (51)$$

In order to obtain unity d.c. gain, the low-pass filter $q(s)$ is chosen as

$$q(s) = q_p(s) e^{\tau_q s} = \frac{a_0}{s^2 + a_1 s + a_0} e^{7.5 \times 10^{-6} s} \quad (52)$$

Phase advance is also added to this low-pass filter for phase cancellation. Thus, a decrease in the steady state error is aimed. The regions in the a_0 - a_1 controller parameter space are computed for three cases which are respectively the nominal performance at low frequencies ($W_T = 0$), robust performance at intermediate frequencies ($W_s \neq 0$ and $W_T \neq 0$) and robust stability at high frequencies ($W_s = 0$).

The sensitivity constraints are specified in COMES at a set of discrete frequencies. The periodic input command of the high speed AFM scanner has a period of 0.0005sec. The specific numerical values of the chosen weights used in the computation of the controller parameters are seen in the table given in Figure 10. The intersection of the regions, which are calculated in order for the nominal performance, the robust performance and the robust stability requirements, in the a_0 - a_1 controller parameter space are filled with green color. The procedure is concluded by choosing a point in the a_0 - a_1 controller parameter plane given in Figure 10.

7 CONCLUSION

The main purpose of this research was to develop an interactive computer program called COMES prepared as a toolbox with a GUI in MATLAB in order to design controllers for mechatronic systems. This toolbox brings together many different control strategies like classical control, preview control, model regulator control and repetitive control. Some of these controller tuning techniques include robust parameter space design. The toolbox offers the users the option to choose one of these control strategies to build a controlled mechatronic

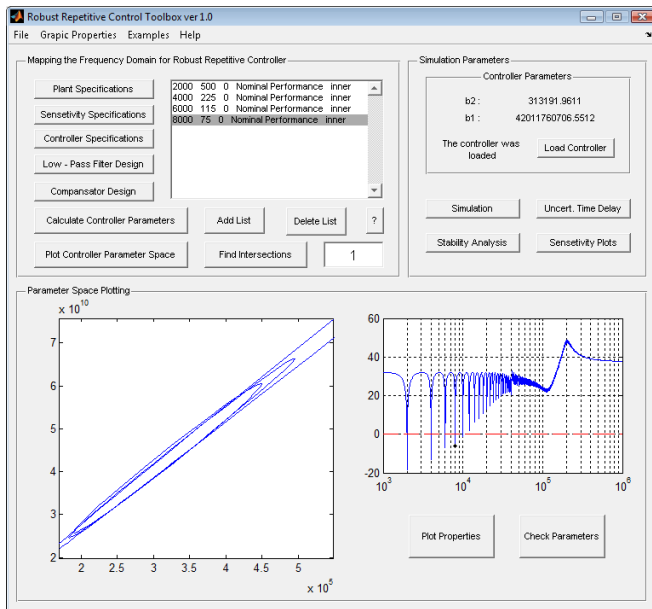


Figure 10. A screenshot of the repetitive control part of the COMES toolbox.

system without having to carry out extensive calculations. Moreover, the effectiveness of the use of this MATLAB-based toolbox was demonstrated by carrying out some design and simulation studies for several position control application available in the literature. The COMES toolbox was successfully classroom tested in a graduate level course on controller design for mechatronic systems in the interdisciplinary Mechatronics graduate program at İstanbul Technical University. Only the repetitive controller design part

of COMES was available during the first classroom testing. The full toolbox was tested the second time. COMES is also being used by members of Mekar labs. The toolbox is under continuous development and will soon be made available to the public.

REFERENCES

- [1] Url-1 <<http://en.wikipedia.org/wiki/Mechatronics>>, accessed at 24.09.2009.
- [2] Isermann R., 2005, *Mechatronic Systems Fundamentals*, Springer Verlag: London, UK.
- [3] Jia L. and Schaufelberger W., 1995, *Software for Control Engineering Education*, Verlag der Fachvereine an der ETH-Zürich, Zürich.
- [4] Johansson M., Gäfvert M. and K.J. Åström K.J., 1998, "Interactive tools for education in automatic control", *IEEE Transactions on Interactive Learning*, pp. 33-40.
- [5] Azemi A. and Yaz E.E., 1997, "Using MATLAB in a graduate electrical engineering optimal control course", *IEEE Frontiers in Education Conference*, pp. 13-17.
- [6] Sienel W., Bünte T. and Ackermann J., 1996, "PARADISE – Parametric robust analysis and design interactive software environment: A Matlab-based robust control toolbox", *IEEE International Symposium on Computer-Aided Control System Design*, pp. 380-385, Dearborn MI.
- [7] Sakabe K., Yanami H., Anai H. and Hara S., 2004, "A MATLAB toolbox for robust control synthesis by symbolic computation", *SICE Annual Conference in Sapporo*, pp. 1968-1973, Japan.
- [8] Hyodo N., Hong M., Yanami H., Anai H. and Hara S., 2006, "Development of a MATLAB toolbox for parametric robust control – algorithms and functions", *ISICE-ICASE International Joint Conference*, pp. 2856-2861, Busan, Korea.
- [9] Balas G.J., A.K. Packard A.K., Safonov M.G. and Chiang R.Y., 2004, "Next generation of tools for robust control", *Proceedings of the 2004 American Control Conference*, pp. 5612-5615, Boston, Massachusetts.
- [10] Vivero O. and Liceago-Castro J., 2008, "MIMO toolbox for Matlab", *Annual IEEE Student Paper Conferece*, pp. 1-5, Aalborg, Denmark.
- [11] Boyle J.M., Ford M.P. and Maciejowski J.M., 1989, "A multivariable toolbox for use with matlab", *IEEE Control System Magazine*, Vol. 9 (1), pp. 59-65.
- [12] Campa G., Davini M. and Innocenti M., 2000, "MVTOOLS: Multivariable systems toolbox", *Proceedings of the 2000 International Symposium on Computer-Aided Control System Design*, pp. 163-167, Anchorage, Alaska, USA.
- [13] Ogata K., 1990, *Modern Control Engineering*, Prentice Hall: New York, USA.
- [14] Thaler G. and Brown R., 1953, *Servomechanism Analysis*, McGraw-Hill: New York, USA.
- [15] Del Toro V. and Parker S., 1960, *Principles of Control Systems Engineering*, McGraw-Hill: New York, USA.
- [16] D'Azzo J. and Houpis C., 1966, *Feedback Control System Analysis and Synthesis*, McGraw-Hill: New York, USA.
- [17] Watkins B., 1969, *Introduction to Control Systems*, Macmillan: New York, USA.
- [18] Dorf R., 1974, *Modern Control Systems*, Addison-Wesley: Reading, MA, UK.

- [19] Ross E., Warren T. and Thaler G., 1960, "Design of servo compensation based on the root locus approach", *AIEE Transactions on Application to Industry*, Vol. **79**, pp. 272-277.
- [20] Wakeland W., 1967, "Analytic technique for root locus compensation with quadratic factors", *IEEE Transactions on Automatic Control*, Vol. **AC-12**, pp. 631-632.
- [21] Wakeland W., 1967, "New analytic technique for root locus compensation", *Proceedings of First Asilomar Conference of Circuits and Systems*, pp. 562-572.
- [22] Wakeland W., 1975, "Bode compensator design", *IEEE Transactions on Automatic Control*, Vol. **AC-21**, pp. 771-773.
- [23] Mitchell J.R., 1977, Comments on "Bode compensator design", *IEEE Transactions on Automatic Control*, Vol. **AC-22**, pp. 869-870.
- [24] Ackermann J., Blue P., Bunte T., Güvenç L., Kaesbauer D., Kordt M., Mühler M., Odenthal D., 2002, *Robust Control: The Parameter Space Approach*, Springer Verlag: London, UK.
- [25] Djaferis T.E., 1991, "Representations of controllers that achieve robust performance for systems with real parameter uncertainty", *Systems and Control Letters*, Vol. **16**, pp. 329-339.
- [26] Saeki M., 1994, "A design method of the optimal PID controller for a two disc type mixed sensitivity problem", *Transactions on the Inst. of Sys. Contr. Info. Eng.*, Vol. **7** (12), pp. 520-527.
- [27] Besson V. and Shenton A.T., 1997, "Interactive control system design by a mixed H-infinity parameter space method", *IEEE Transactions on Automatic Control*, Vol. **42**, pp. 946-955.
- [28] Bunte T., 1998, "Beitrag zur robusten lenkregelung von personenkraftwegen", Ph.D: Dissertation, RWTH Aachen, VDI Fortschritt-Bericht, Reihe 12, Nr. 366, VDI-Verlag, Düsseldorf.
- [29] Odenthal D. and Blue P., 2000, "Mapping of H-infinity design specifications into parameter space", *Proceedings of 3rd IFAC Symposium on Robust Control Design*, Prague.
- [30] Saeki M. and Hirayama D., 1996, "Parameter space design method of PID controller for robust sensitivity minimization problem", *Transactions on the Society of Instrument and Control Engineers*, Vol. **32** (12), pp. 1612-1619.
- [31] Saeki M. and Kimura J., 1998, "Design method of robust PID controller and CAD system", *Proceedings of the 11th IFAC Symposium on System Identification*, Vol. **3**, pp. 1587-1593.
- [32] Saeki M., 2006, "Fixed structure PID controller design for standard H-infinity control problem", *Automatica*, Vol. **42** (1), pp. 93-100.
- [33] Besson V. and Shenton A.T., 1999, "An interactive parameter space method for robust performance in mixed sensitivity problems", *IEEE Transactions on Automatic Control*, Vol. **44**, pp. 1272-1276.
- [34] Güvenç L. and Ackermann J., 2001, "Links between the parameter space and frequency domain methods of robust control", *International Journal of Robust and Nonlinear Control*, Vol. **11** (15), pp. 1435-1453.
- [35] Ackermann J., Guldner J., Sienel W., Steinhauser R. and Utkin V.I., 1995, "Linear and nonlinear controller design for robust automatic steering", *IEEE Transactions on Control Systems Technology*, Vol. **3** (1), pp. 132-143.
- [36] Cannon R.H. and Schmitz E., 1984, "Initial experiments on the control of a flexible manipulator", *International Journal of Robotics Research*, Vol. **3**, pp. 62-75.
- [37] Tomizuka M., 1987, "Zero phase error tracking algorithm for digital control", *ASME Journal of Dynamic Systems, Measurement and Control*, Vol. **109** (1), pp. 65-68.
- [38] Haack B. and Tomizuka M., 1991, "The effect of adding zeros to feedforward controllers", *ASME Journal of Dynamic Systems, Measurement and Control*, Vol. **113** (1), pp. 6-10.
- [39] Menq C.H. and Xia Z., 1990, "Characterization and compensation of discrete-time nonminimum phase zeros to feedforward controllers", *Proceedings of ASME Symposium on Robotics Research*, DSC-Vol. **26**, pp. 15-23, New York.
- [40] Aksun Güvenç B. and L. Güvenç L., 1999, "Optimal precision tracking control of discrete time nonminimum phase systems", *Proceedings of European Control Conference*.
- [41] Güvenç L., Harib K. and Srinivasan K., 1995, "Extended precision tracking control of discrete-time nonminimum phase systems", *Proceedings of ASME International Mechanical Engineering Congress and Exposition*, DSC-Vol. **57** (1), pp. 151-158, San Fransisco.
- [42] Gross E., Tomizuka M. and Messner W., 1994, "Cancellation of discrete time unstable zeros by feedforward control", *ASME Journal of Dynamic Systems, Measurement and Control*, Vol. **116** (1), pp. 33-38.
- [43] Åström K.J., Hagender P. and Sternby J., 1984, "Zeros of sampled systems", *Automatica*, Vol. **20**, pp. 31-38.
- [44] Aksun Güvenç B. and Güvenç L., 2001, "Characterization and compensation of complex nonminimum phase zeros for preview control", *IEEE Mediterranean Conference on Control and Automation*.
- [45] Fu Y. and Dumont G.A., 1989, "Choice of sampling to ensure minimum-phase behaviour", *IEEE Transactions on Automatic Control*, Vol. **34** (5), pp. 560-563.
- [46] Ishitobi M., 1992, "Conditions for stable zeros of sampled systems", *IEEE Transactions on Automatic Control*, Vol. **37** (10), pp. 1558-1561.
- [47] Tsao T.C. and M. Tomizuka M., 1994, "Robust adaptive and repetitive digital control and application to a hydraulic servo for noncircular machining", *ASME Journal of Dynamic Systems, Measurement and Control*, Vol. **116** (1), pp. 24-32.
- [48] Ohnishi K., 1987, "A new servo method in mechatronics", *Transactions on Japanese Electrical Engineers*, Vol. **107-D**, pp. 83-86.
- [49] Umeno, T. and Hori, Y., 1991, "Robust Speed Control of DC Servomotors Using Modern Two Degrees-of-Freedom Controller Design", *IEEE Transactions on Industrial Electronics*, Vol. **38** (5), pp. 363-368.
- [50] Kempf C.J. and Kobayashi S., 1999, "Disturbance observer and feedforward design for a high-speed direct-drive positioning table", *IEEE Transactions on Control Systems Technology*, Vol. **7** (5), pp. 513-526.
- [51] Güvenç L. and Srinivasan K., 1994, "Friction compensation and evaluation for a force control application", *Mechanical Systems and Signal Processing*, Vol. **8** (6), pp. 623-638.
- [52] Aksun Güvenç B., Bunte T., Odenthal D. and Güvenç L., 2004, "Robust two degree of freedom vehicle steering compensator design", *IEEE Transactions on Control Systems Technology*, Vol. **12** (4), pp. 627-636.
- [53] Bunte T., Odenthal D., Aksun Güvenç B. and Güvenç L., 2002, "Robust vehicle steering control based on the disturbance observer", *IFAC Annual Reviews in Control*, part 1, Vol. **26**, pp. 139-149.
- [54] Karaman S., Öncü S., Güvenç L., Ersolmaz Ş.S., Çetin E., Kanbolat A., 2006, "Robust Velocity Scheduled Yaw Stability Control of a Light Commercial Vehicle", *IEEE Intelligent Vehicles Symposium*, Tokyo.

- [55] Öncü S., Karaman S., Güvenç L., Ersolmaz S., Öztürk E., Çetin E., Sinal M., 2007, "Robust Yaw Stability Controller Design for a Light Commercial Vehicle Using a Hardware in the Loop Steering Test Rig", *IEEE Intelligent Vehicles Symposium*, Istanbul.
- [56] Francis B.A. and Wonham W.M., 1975, "The internal model principle for linear multivariable regulators", *Applied Mathematics and Optimization*, Vol. **2**, pp. 170-194.
- [57] Inoue T., Iwai S., and Nakano M., 1981, "High accuracy control of a proton synchrotron magnet power supply", *Proceedings of 8th IFAC World Congress*, Part 3, pp. 3137-3142.
- [58] Cheng Y.Q., Moore K.L., Yu J. and Zhang T., 2004, "Iterative learning control and repetitive control in hard disk drive industry – a tutorial".
- [59] Moon J.H., Lee M.N., and Chung M., 1998, "Repetitive control for the track-following servo system of an optical disk drive", *IEEE Transactions on Control Systems Technology*, Vol. **6** (5), pp. 663-667.
- [60] Omata T., Hara S., and Nakano M., 1987, "Nonlinear repetitive control with application to trajectory control of manipulators", *Journal of Robotic Systems*, Vol. **4** (5), pp. 631-652.
- [61] Sadegh N., Horowitz R., Kao W.W., and Tomizuka M., 1990, "A unified approach to the design of adaptive and repetitive controllers for robotic manipulators", *ASME Journal of Dynamical Systems, Measurement and Control*, Vol. **112** (4), pp. 618-629.
- [62] Kobayashi F., Hara S., and Tanaka H., 1990, "Reduction of motor speed fluctuation using repetitive control", *Proceedings of 29th IEEE Conference on Decision and Control*, pp. 1697-1702.
- [63] Fung R.F., Huang J.S., and Chien C.C., 2000, "Design and application of a continuous repetitive controller for rotating mechanisms", *International Journal of Mechanical Sciences*, Vol. **42** (9), pp. 1805-1819.
- [64] Shaw F.R., and Srinivasan K., 1993, "Discrete-time repetitive control systems design using the regeneration spectrum", *ASME Journal of Dynamical Systems, Measurement and Control*, Vol. **115** (2A), pp. 228-237.
- [65] Garimella S.S., and Srinivasan K., 1996, "Application of repetitive control to eccentricity compensation in rolling", *ASME Journal of Dynamical Systems, Measurement and Control*, Vol. **118** (4), pp. 657-664.
- [66] Tinghsu S., Hattori S., Ishida M., and Hori T., 2002, "Suppression control method for torque vibration of AC motor utilizing repetitive controller with fourier transform", *IEEE Transactions on Industry Application*, Vol. **38** (5), pp. 1316-1325.
- [67] Rech C., Pinheiro H., and Grudling H., 2003, "Comparison of digital control techniques with repetitive integral action for low cost PWM inverters", *IEEE Transactions on Power Electronics*, Vol. **18** (1), pp. 401-410.
- [68] Zhang K., Kang Y., and Xiong J., 2003, "Direct repetitive control of SPWM inverter for UPS purpose", *IEEE Transactions on Power Electronics*, Vol. **18** (3), pp. 784-792.
- [69] Zhou K., and Wang D., 2003, "Digital repetitive controlled three-phase PWM rectifier", *IEEE Transactions on Power Electronics*, Vol. **18** (1), pp. 309-316.
- [70] Choi G.S., Lim Y.A., and Choi G.H., 2002, "Tracking position control of piezoelectric actuators for periodic reference inputs", *Mechatronics*, Vol. **12** (5), pp. 669-684.
- [71] Choi G.H., Jong H.O., and Choi G.S., 1999, "Repetitive tracking control of a coarse-fine actuator", *Proceedings of IEEE/ASME International Conference Advanced Intelligent Mechatronics*, pp. 335-340.
- [72] Hara S., Yamamoto Y., Omata T. and Nakano M., 1988, "Repetitive control systems: A new type servo system for periodic exogenous signals", *IEEE Transactions on Automatic Control*, Vol. **33**, pp. 657-667.
- [73] Srinivasan K., and Shaw F.R., 1991, "Analysis and design of repetitive control systems using the regeneration spectrum", *ASME Journal of Dynamical Systems, Measurement and Control*, Vol. **113** (2), pp. 216-222.
- [74] Tomizuka M., Tsao T.C., and Chew K.K., 1989, "Analysis and synthesis of discrete-time repetitive controllers", *ASME Journal of Dynamical Systems, Measurement and Control*, Vol. **111** (3), pp. 353-358.
- [75] Srinivasan K., Özbay H., and Jung I.S., 1995, "A design procedure for repetitive control systems", *Proceedings of ASME International Mechanical Engineer's Congress and Exposition*, pp. 581-593.
- [76] Özbay H., 1993, " H_∞ optimal controller design for a class of distributed parameter space", *International Journal of Control*, Vol. **58** (4), pp. 739-782.
- [77] Peery T. and Özbay H., 1997, " H_∞ optimal repetitive controller design for stable plants", *ASME Journal of Dynamical Systems, Measurement and Control*, Vol. **119** (3), pp. 541-547.
- [78] Roh C.L. and Chung M.J., 1995, "Design of repetitive control system for an uncertain plant", *Electronics Letter*, Vol. **31** (22), pp. 1959-1960.
- [79] Weiss G. and Häfele M., 1999, "Repetitive control of MIMO systems using H_∞ design", *Automatica*, Vol. **35**, pp. 1185-1199.
- [80] Weiss G., Zhong Q.Z., Green T.C. and Liang J., 2004, " H_∞ repetitive control of DC-AC converters in microgrids", *IEEE Transactions on Power Electronics*, Vol. **19** (1), pp. 219-230.
- [81] Zhong Q.C., Liang J., Weiss G., Feng C. and Green T.C., 2006, " H_∞ control of the neutral point in four-wire three-phase DC-AC converters", *IEEE Transactions on Industrial Electronics*, Vol. **53** (5).
- [82] Doh T.Y. and Chung M.J., 2003, "Repetitive control design for linear system with time-varying uncertainties", *IEEE Proceedings of Control Theory Applications*, Vol. **150**, pp. 427-432.
- [83] Güvenç L., 1996, "Stability and performance robustness analysis of repetitive control systems", *ASME Journal of Dynamical Systems, Measurement and Control*, Vol. **118** (3), pp. 593-597.
- [84] Li J. and Tsao T.C., 1998, "Robust performance repetitive control design using structured singular values", *Proceedings of ASME International Mechanical Engineer's Congress and Exposition*.
- [85] Aksun Güvenç B. and Güvenç L., 2006, "Robust repetitive controller design in parameter space", *ASME Journal of Dynamical Systems, Measurement and Control*, Vol. **128**, pp. 406-413.
- [86] Omata T., Hara S., and Nakano M., 1985, "Synthesis of repetitive control systems and its applications", *Proceedings of IEEE Conference on Decision and Control*, pp. 1387-1392.
- [87] Sadegh N., 1991, "Synthesis and stability analysis of repetitive controllers", *Proceedings of American Control Conference*, pp. 2634-2639.
- [88] Hara S., 1988, "Repetitive control system: a new type of servo for periodic exogenous signals", *IEEE Transactions on Automatic Control*, Vol. **33** (7), pp. 659-668.
- [89] Hara S. and Yamamoto Y., 1985, "Stability of repetitive control systems", *Proceedings of IEEE Conference on Decision and Control*, pp. 326-327.

- [90] Silva G.J., A. Datta A., Bhattacharya S.P., 2005, *PID Controllers for Time-delay Systems*, Boston: Birkhäuser.
- [91] El'sgol L.E., 1966, *Introduction to the theory of differential equations with deviating argument*, Translated by R. J. McLaughlin Holden-day, San Francisco.
- [92] Srinivasan K. and Nachtigal C.L., 1978, "Analysis and design of machine tool chatter control systems using regeneration spectrum", *ASME Journal of Dynamical Systems, Measurement and Control*, Vol. **100**, pp. 191-200.
- [93] Bartalucci B. and Lucci G.G., 1969, "Grinding process instability", *ASME Journal of Engineering and Industry*, Vol. **19**, pp. 597-606.
- [94] Broberg H.L. and Molyet R.G., 1994, "A new approach to phase cancellation in repetitive control", *Proceedings of Industry Applications Society Annual Meeting*, Vol. **3**, pp. 1766-1770.
- [95] Schitter G., Åström K.J., DeMartini B.E., Thurner P.J., Turner K.L. and Hansma P.K., 2007, "Design and modelling of a high-speed AFM-scanner", *IEEE Transactions on Control Systems Technology*, Vol. **15** (5), pp. 906-915.
- [96] Demirel, B., 2009, "Interactive Computer-Aided Controller Design for Mechatronic Systems," M.S. Thesis, Istanbul Technical University, Istanbul, Turkey.